Comparing the Alberta Taciuk Processor and the Shell In Situ Conversion Process - Energy Inputs and Greenhouse Gas Emissions

Adam R. Brandt

Energy and Resources Group, University of California, Berkeley

Abstract

This paper compares the Shell in situ conversion process (ICP) to the Alberta Taciuk Processor (ATP) using metrics of energy efficiency and carbon dioxide emissions.

The ICP is an experimental method of retorting oil shale without removing it from the earth. The ICP utilizes electricity to heat the underground shale slowly over a period of 2 years. The generated hydrocarbons are then produced using conventional oil production techniques, leaving the shale oil coke within the formation. This study modeled the energy inputs and outputs, and the greenhouse gas (GHG) emissions from two possible implementations of the ICP, as applied to oil shale of the Green River formation of western Colorado.

The Alberta Taciuk Processor (ATP) is an above-ground oil shale retort. The ATP retort requires less external fuel input than other above-ground retort designs, because it combusts the coke or "char" deposited on the shale during retorting to provide heat to the retorting process. However, this requires combustion of the spent shale, potentially increasing temperatures high enough to induce carbonate decomposition, thus liberating additional CO_2 from minerals in the shale. This paper reports modeling of two cases of ATP deployment.

Results suggest that primary energy inputs per unit of energy output range from 0.46 to 0.73 megajoules (MJ) per MJ of final fuel delivered for the ICP process and from 0.36 to 0.59 MJ/MJ for the ATP process. For the ICP, upstream greenhouse gas emissions range from 7.7 to 16.6 grams of carbon equivalent per MJ final fuel delivered, whereas emissions from the ATP range from 34 to 42 gCeq/MJ FFD, depending on the ATP operation. These emissions are roughly 10% to 70% higher than those from conventionally produced petroleum-based fuels on a full fuel cycle basis.

Introduction

Oil shale is seen as a potential "backstop" resource, or a resource that will be used when conventional reserves of oil are depleted [Bartis et al., 2005]. This is for two reasons: it is abundant and it is domestically available [Johnson et al., 2004]. Unfortunately, oil shale production entails a heavy environmental burden, with traditional methods of production emitting high levels of criteria air pollutants, greenhouse gases (GHGs), and water pollutants [OTA, 1980; Sundquist and Miller, 1980].

There are two types of oil shale retorting processes: above ground and in situ. Above-ground processes require mining the shale and processing it in an above-ground retort. In situ processes convert the kerogen to hydrocarbons by applying heat to shale in place. Previous oil shale operations, largely in Australia, Estonia, the United States, and China [Dyni, 2006], have been above-ground, whereas in situ processes are in active development [Bartis et al., 2005].

Recent interest in oil shale R&D has been spurred by federal support for oil shale development [BLM, 2006]. Of particular importance to this paper are three proposals submitted by Shell [Shell, 2006a, b, c] and a proposal by Oil Sands Exploration Company (OSEC), all submitted in response to a Bureau of Land Management call for research proposals [BLM, 2006; OSEC, 2006].

This paper outlines necessary background information about the ICP, then describes

the modeling philosophy for low and high energy and GHG intensity ICP cases (hereafter the "low" and "high" primary cases). In the working papers from which this paper is adapted (available at http://abrandt.berkeley.edu/), detailed process-stage methodologies are presented and higher and lower "boundary cases" are also examined. These details are omitted here due to space constraints. The paper repeats this analysis for the ATP-based processes. Results for both processes are presented using two summary statistics: energy inputs per megajoule (MJ) of final fuel delivered (FFD), and GHG emissions per MJ of FFD.

The in-situ conversion process

ICP Background

The ICP is significantly different from previously implemented oil shale production processes, and can be classified as a true in situ process [Burnham and McConaghy, 2006]. In the ICP, a freeze wall is first created around the perimeter of an area of shale to be retorted (called here the production "cell"). Next, heat is transferred to the oil shale in place within the cell. In current designs, this heat is provided by electric resistance heating. The applied heat conducts through the formation, slowly heating the shale to the temperature of kerogen decomposition. As the shale is converted, the resulting hydrocarbons are pumped from the earth. Lastly, the production cell is remediated: any remaining mobile hydrocarbons are flushed from the earth and the freeze wall is thawed.

Both cases modeled in this paper are large-scale implementations of the ICP, but they are based heavily on the Oil Shale Test Project (OST), a subcommercial- scale test of the ICP. The OST is documented in detail in the Plan of Operations (PO) submitted by Shell to the Bureau of Land Management [Shell, 2006c], as well as a detailed 7-volume mining operation reclamation permit application, submitted to the Colorado Division of Reclamation and Mining Safety (hereafter mining permit application or MPA) [Shell, 2007].

The ICP is also documented in many of patents, totaling thousands of pages. Information in these patents is not generally useful for reconstructing the ICP. The patents describe a number of variations of the ICP: some produce hydrogen instead of hydrocarbons, others produce arbitrary mixtures of hydrocarbon gases and hydrogen [Berchenko, et al. 2006, p. 406], and still others could be applied to deep coal seams [Berchenko, et al.,2006; Vinegar, personal communication, 2007] or tar sands deposits [Vinegar, personal communication, 2007]. Despite the variety in potential applications, only a simplified "generic" ICP, as described in the PO and MPA are modeled here. The steps of this ICP are described below in order of execution.

Siting and preliminary operations: A production area is chosen based on a number of characteristics. A thick shale formation increases yield per unit of input. The formation should have less-permeable layers on top and bottom to prevent flux of water into, or hydrocarbons out of, the cell [Shell, 2007]. In the PO, the formation targeted lies under 271 m of inert overburden, and the total thickness of shale is 318 m [Shell, 2006c]. The OST PO states that all of this thickness is to be treated, but the more recent MPA states that only two layers of the shale formation will be converted [Shell, 2007, Appendix 22, p. 8].

A production cell is prepared by constructing above-ground facilities, tanks, access roads, drilling pads, etc. The layout of production cells in both the OST and in the three cases modeled is shown in Figure 1. The dimensions of the production cell are important. Larger cells have significant economic advantages: the amount of perimeter per unit of shale retorted becomes significantly smaller in larger cells, reducing heat losses and lowering the amount of energy expended in creating the freeze wall. This effect makes the efficiency and GHG implications of OST-scale develop-

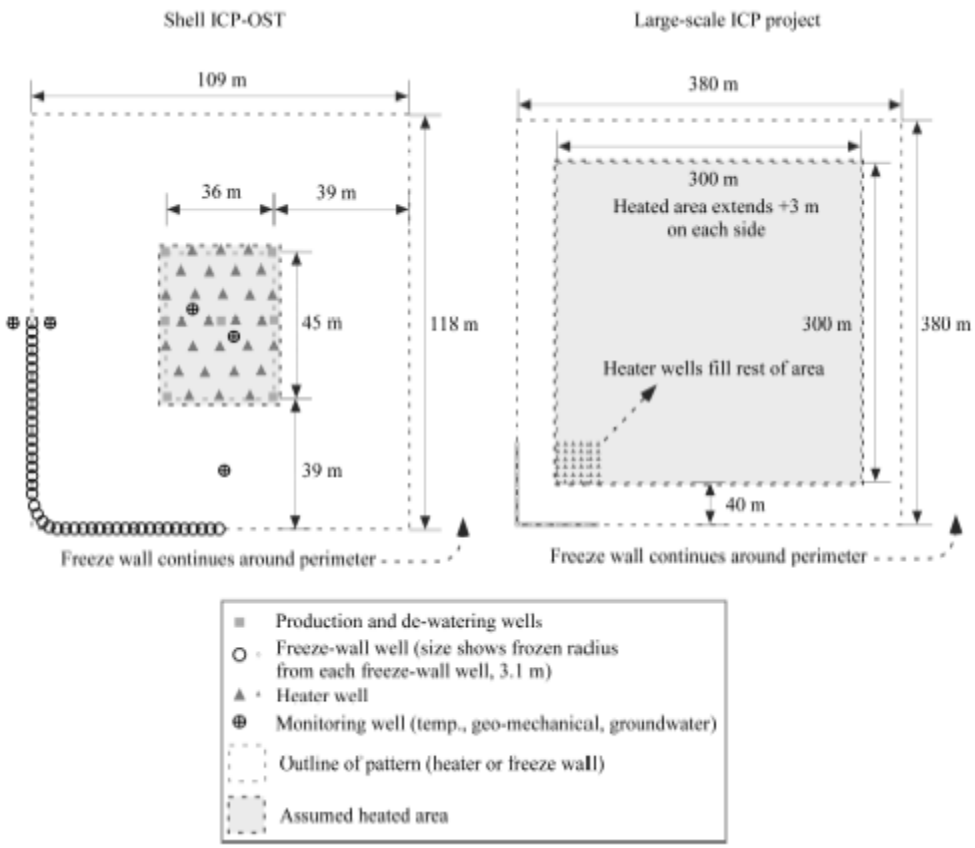

Figure 1: Well schematic for two configurations of the ICP: OST (left, adapted from Shell, 2006c) and three modeled full-scale cases (right). Heated area extends slightly beyond heater well pattern. Not all monitoring wells are shown.

ments significantly different from those of large-scale ICP development.

As shown in Figure 1, the OST uses a cell with a heater well pattern area of ~1600 m^2, whereas cases modeled in this study use a heater well pattern of 300 m by 300 m, or 90,000 m^2. It is unclear how large a cell could be made in practice, given the topography of the area of development as well as subsurface heterogeneity that might limit the size of cells (e.g. faults). Burnham suggests that kilometer-scale projects are possible [Burnham, personal communication, 2007].

Freeze wall construction: A single ring of wells is drilled around the cell. Internal and external casing is inserted into these wells and refrigerant is circulated through the wells at approximately -40 °C [Shell, 2006c]. This forms a freeze wall, an underground vertical wall of frozen soil and rock, over a period of 1.5 to 2 years. In the OST, freeze wall wells are placed at intervals of approximately 2.5 m [Shell, 2006c, p. 4-8]. This is a design parameter: if a cooler working fluid is used, the freeze wall will be thicker after it stabilizes, allowing the wells to be drilled further apart and reducing drilling costs [Berchenko, et al., 2006, p. 394]. In the OST, the final wall is 3.1 m thick [Mut, in U. S. Senate, 2005].

The freeze wall prevents produced hydrocarbons from escaping from the cell and prevents additional ground water from infiltrating the cell. Some sources suggest that a double ring of freeze wall wells can be required to prevent intrusion of water [Sanger et al., 1979, p. 322].

The freeze wall is maintained throughout the life of the project, likely extending 6.5 years [Shell, 2007, p. 3-16] to 8 years [Shell, 2006c] after formation. The lower-permeability layers above and below the treated shale combine with the freeze wall

to isolate the cell, in theory preventing mixing of oil and water [Shell, 2006c]. Shell is currently testing the ability of the freeze wall to resist pressure gradients and the ability to repair the wall after a breach [Vinegar, personal communication, 2007].

Water removal: Wells are drilled in the cell interior. These wells are first used to "de-water" the cell, removing mobile water from pores and fractures in the shale. Because water has a high heat capacity, 4.18 J/g-°C vs. about 1 J/g-°C for oil shale [Hendrickson, 1975], the economics of production require that as much water as possible be removed from the shale. Produced water is re-injected outside of the cell [Shell, 2006c].

The OST shale exists well below the water table, and all porosity is filled with water [Shell, 2007]. At the OST site, total porosity and drainable or "effective" porosity, averaged by depth, are 10.7 and 3.8%, respectively [Shell, 2007, Appendix 21, p. 10]. Thus, after removal of all drainable water, water will occupy 6.9% of cell bulk volume.

Heating: Heater wells are drilled at close spacing in the cell and electric heaters are inserted into the wells. The distance between the wells is flexible, and they are drilled at a spacing of 7.8 m in the OST [Shell, 2006c]. The spacing of heater wells is a tradeoff: closer well spacing allows the shale to be heated more quickly but increases the costs [Burnham and McConaghy, 2006]. The heating elements are designed to maintain a high but constant temperature without being damaged by excessive heat [U. S. Senate, 2005; Shell, 2006c; Vinegar, et al., 2004]. These heaters are operated so as to heat the oil shale to temperatures between 340°C and 400 °C [U. S. Senate, Mut testimony; Shell, 2006c] as shown in Figure 2.

The rate and duration of heating can vary. In the OST, heating occurs over 2 years [Shell, 2006c, p. 4-13], whereas an earlier test project was heated in 1 year [Berchenko, et al., 2006]. After heating ceases, production continues for some time. There is some uncertainty in the time of heating, as the newer MPA suggests that the OST will be brought to final temperature in 2 years, but that heating will occur for about 3 years [Shell, 2007, p. 4-5]. This is

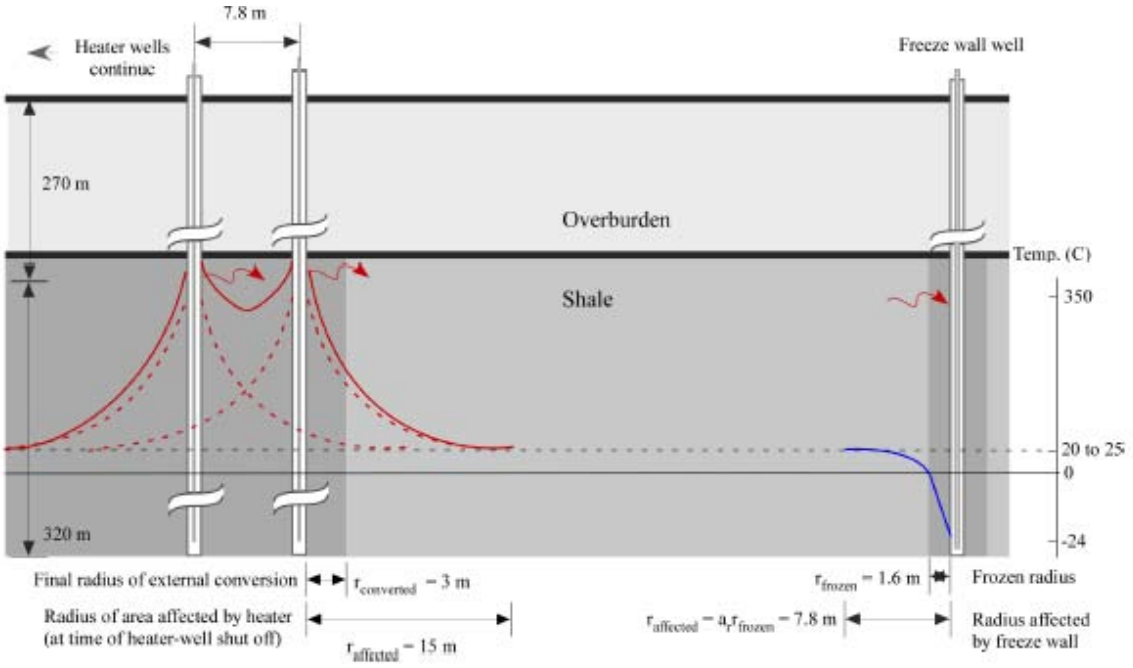

Figure 2: Illustrative temperature profiles in ICP. Lateral distance affected by heater well is assumption for time of heater-well shut off (see discussion below), and the radius of conversion includes conversion that occurs after heater-well shut off.

somewhat at odds with non-isothermal kerogen conversion models which do not suggest the need for "soaking" at high temperature (conversion is complete after the final temperature is reached), nor is it compatible with plots of temperature from other ICP tests, which show temperature increasing roughly linearly until heaters are shut off, then immediately decreasing [Berchenko, et al., 2006, Fig. 188].

The rate of heating is a key parameter because the temperature at which oil formation is complete varies with the rate of heating [Burnham, 1993; Burnham and McConaghy, 2006]. At atmospheric pressure and 3 °C increase per month, kerogen conversion is essentially complete at 300 °C, whereas at 3 °C increase per day, conversion is complete at 350 °C [Burnham, 1993; Burnham and McConaghy, 2006]. Because of this difference, it is more thermally efficient to heat the kerogen slowly [Burnham and McConaghy, 2006]. The rate of heating implied by the OST PO and the MPA is approximately 0.5 °C per day (~ 350 °C increase over a two year period).

The ICP converts kerogen at elevated pressures. Pore pressure during conversion is determined by the balance between pressure generated by the vaporization of produced gas and oil products and pressure relieved as these products move to the lower-pressure production wells [Burnham, personal communication, 2007]. One cited pressure range is between 2 and 35 atm [Berchenko, 2006]. As an upper limit, pore pressure cannot exceed the lithostatic pressure (pressure applied to pore space from the overlying rocks), as this would cause fracturing of the formation. Also, pore pressure is limited in the OST to less than 27 atm at the top of the formation by the expected strength of the freeze wall [shell, 2007, Appendix 16, p. 47].

Heat loss to the over-burden is likely to be minor. The shale layer is 320 m deep, whereas the effective radius of heating of each well is on order 5-10 m. Thus, the surface area of a cylinder of heating is about two orders of magnitude larger on the sides than the top or bottom, even when the heated area is at its fullest extent. Also, thermal conductivities of sedimentary rocks and shale are anisotropic, such that conduction is more efficient along the layers of shale ("bedding planes") than perpendicular to them [Clauser and Huenges, 1995; Hendrickson, 1995]. Shell models confirm this intuition, showing a temperature increase of 17 °C at a point 16 m above the top of the heated layer [Shell, 2007, Appendix 16, p. 32].

Heating will also occur laterally outside of the heater-well pattern, and heat will be wasted in shale that never reaches conversion temperature. In Shell tests using a small pattern on 2.6 m spacing, conversion was seen on cores 0.6 m outside of the pattern [Berchenko, et al., column 239]. In models of the OST, conversion is predicted 3-5 m outside of pattern after 900 days [Shell, 2007, Appendix 22, p. 10]. Thus, waste heating begins a few meters outside of the heater well pattern and extends laterally toward the four freeze walls. The freeze wall is placed sufficiently far away that heat from the heater wells will not appreciably reach the freeze wall [Shell, 2006c].

Recoverable oil in place The amount and type of hydrocarbons produced from the ICP are uncertain, and published figures are in some disagreement [Burnham and McConaghy, 2006]. Oil shale yields are quoted relative to yields obtained by subjecting the shale to a defined retorting process: the Fischer Assay (FA). Shell suggests that recovery is 100% of FA yield in terms of BOE (barrels of oil equivalent) [Shell, 2006c]. This figure must include gas as well as oil because all other sources suggest that oil yield is lower at lower temperatures and higher pressures, both of which apply to the ICP [Burnham, 2003; Burnham and McConaghy, 2006; Hendrickson, 1995]. Also, data extracted from figures in a Shell patent show an oil yield of 80 vol.% of FA yield from a heating rate of 0.5 °C/d [Berchenko, et al., 2006, Fig. 197].

Gas yield from the ICP will be higher than FA gas yield, because slower heating re-

sults in more gas production [Burnham, 2003; Burnham and Singleton, 1983]. Higher pressure also tends to increase gas yield. Burnham and Singleton report 1.7 times FA gas yield at pressures of 27 atm, although they had trouble accounting for all carbon from the kerogen, possibly due to gas leaks or excess gas dissolved in liquid phase oil [Burnham, 2003]. If the missing carbon in those data is added to the gas yield, the yield of gas becomes ~ 2 to 2.5 times that of the FA yield [Burnham and Singleton, 1983]. Combining Shell statements regarding overall energetic yield and oil-gas balance implies a higher gas yield of about 3.5 times FA.

Lastly, Shell does not state if these yield figures represent oil generated or oil actually produced from the well bore. Oil generated travels to production wells in the vapor phase, reducing the potential for trapping. Shell models show low residual hydrocarbon saturation (0-4%) within the body of the heated area [Shell, 2007, Appendix 22, p. 15], and similar efficiency was seen in independent experiments [Burnham, personal communication, 2007]. But oil flushed from the heated area can move toward the perimeter of the cell in addition to moving toward production wells (pressure gradients outside of the heater-well pattern can force oil outward rather than inward, where it condenses as it cools) [Shell, 2007, Appendix 22]. Thus, Shell models show a ring of high residual oil saturation outside of the heated areas (~40%), and it is largely this oil that the flushing process attempts to clean up.

The net effect of this expulsion is uncertain: Berchenko et al. [2006, column 239] state that cores drilled after production from an ICP test show “oil recovery efficiency...in the 75% to 80% range”. Burnham assumed an 80% “expulsion-recovery fraction” when modeling a different in situ process [Burnham, 2003, p. 13].

Production: ICP produces a high grade, light oil with relatively few impurities, because the majority of long-chain heavy hydrocarbons are left in the formation or are converted to coke within the formation. Hydrocarbons travel toward the production wells in vapor form [Berchenko, et al., 2006, Column 241]. The phase of hydrocarbons during production depends on the operation of the ICP. In the OST, the resulting hydrocarbon is pumped from the earth at approximately 200 °C using standard oil production techniques [Shell, 2006c]. At this temperature, a significant fraction of the crude stream is in condensed form [Leffler, 2000]. An earlier Shell test produced hydrocarbons as vapor [Berchenko, et al., 2006].

Restoration and remediation: After oil production ceases to be profitable, the production cell is flushed with water to cool the shale and recover any remaining mobile hydrocarbons [Shell, 2006c, p. 5-1]. The amount of flushing required will vary depending on the nature of the shale residuals and on water quality standards. Shell MPA claims that contaminant concentrations will decrease to allowable limits after flushing with about 20 pore volumes of water [Shell, 2007, p. 11-11].

After water quality targets are met for the production cell, the freeze wall is allowed to thaw. Waste heat could be utilized in a large-scale, multi-cell production operation: hot flush water from a cell undergoing remediation could be pumped into another cell to preheat the formation before the application of electric heating [Vinegar, personal communication, 2007].

Refining: Oil from the OST does not require upgrading, only minor pre-transport processing (desalting and minor distillation to reduce vapor pressure) [Shell, 2006c, p. 4- 18]. It is then sent to a refinery for conversion into finished fuel products.

ICP analysis methods

For this analysis of the ICP, calculations of inputs and outputs are made in a life-cycle assessment framework. Energy inputs and outputs are tabulated and compared for both cases. Greenhouse gas emissions are then calculated for both cases.

Life cycle assessment: A simplified life-cycle assessment is performed for each case, using a process model approach [Ciam-

brone, 1997]. The low and high cases use plausible low and high estimates for inputs (*e.g.* steel input), energy intensity of each input (*e.g.* embodied energy per unit of steel), and yields of oil and gas. Conscious effort was made to choose conservative (low) input and energy intensity estimates.

Labor inputs are not counted, nor are energy inputs or emissions resulting from labor support. Water usage is not estimated. The energy requirements of important primary steel and concrete inputs are estimated, but no other materials energy intensities are included. No secondary materials intensities are calculated (*e.g.* the intensity of steel manufacturing capacity). There is some level of inherent incommensurability between cited studies of individual components that are used in this analysis (*e.g.* steel vs. cement), ensuring that system boundaries can only be adhered to approximately.

For a detailed description of my methods for calculating impacts from each process stage described above, please see working papers cited above.

Comparison of energy inputs and outputs: Using the results from the LCA for each step, the energy inputs are summed for all process steps per tonne of throughput. All electricity is converted to primary thermal energy. These calculations give total primary MJ consumed per tonne of throughput. These are compared to FFD per tonne of throughput, using the following ratio:

$$\eta = \frac{\sum E_{cons}}{\sum E_{prod}} \quad (1)$$

Where: E_{cons} is the total energy consumed in producing the final fuel, and

E_{prod} is the total final fuel energy delivered to users (FFD).

This figure has units of MJ/MJ of FFD, and it shows the amount of energy (from all sources, internal and external to the system) that must be consumed to produce a unit of final fuel output. This figure is comparable to figures reported by Wang et al. as WTP energy use [Wang, et al., 2004, Fig. 3].

Emissions: Energy inputs to each process step (MJ/MJ of FFD) are multiplied by the emissions factor for the fuel consumed in that step, giving grams of carbon equivalent GHGs per MJ of final fuel delivered (gC_{eq}/MJ FFD). In some cases, the fuel used in a process is unclear or not cited, requiring assumptions. The low and high cases are used to create low and high emissions estimates. Emissions factors are given by EIA [EIA, 2003].

The Alberta Taciuk processor

ATP background

In this paper above-ground mine and retort (M&R) processes are modeled using the Alberta Taciuk Processor (ATP). Some sources call this retort the AOSTRA Taciuk Process, after the Alberta Oil Sands Technology and Research Authority, the funding source for its original development as an oil sands processor [Berkovich, et al., 1]. The primary cases studied are two large-scale deployments of the ATP which have low and high energy and GHG intensities. In addition, two bounding cases will be analyzed: a low-temperature large-scale case, where combustion temperatures are lowered to reduce carbon dioxide formation from carbonate mineral decomposition, and a small-scale case based on OSEC Phase 3 parameters.

The paper presents two calculations for each case, as with the ICP: 1) estimated energy inputs and outputs of the production process and calculate the energy input per Megajoule (MJ) of final fuel delivered; 2) the GHG emissions from production of final fuels from oil shale.

The modeled production processes consist of five stages: mining and processing, retorting, disposal of spent shale, on-site upgrading of raw shale oil, and refining of upgraded shale oil.

Mining and processing of raw oil shale: The room-and-pillar method is the technique most likely to be used in underground mining [Bartis, et al. 2005], and

OSEC has proposed using room-and-pillar techniques [OSEC, 2006, p. 30].

Although previous oil shale facilities used underground mines, many believe that a large-scale oil shale industry would rely on open-pit mining. This is because recovery factors are higher and costs are lower for open-pit mining. Underground mining recovery factors can be as low as 10 to 20% for exceptionally thick seams, in which much Green River shale occurs [Bartis, et al. 2005, p. Burnham and Singleton, 1983].

Recovery factors for open-pit mining are higher. Also the thickness of Green River oil shale deposits creates a favorable "stripping ratio" (the ratio of the depth of inert rock overlaying the shale to the depth of shale, which is important for open-pit mining economics). These factors suggest that large-scale operations would use open-pit mines. A plausible size for a commercial operation is 100,000 bbl/d, which would require a 25 million tonne per year mine [Bartis, et al. 2005]. This is approximately 1/3 the capacity of the very large surface coal mines of Wyoming [Bartis, et al. 2005].

After mining, the shale is hauled from the mine to the above-ground processing facility, or retort, where hydrocarbons are extracted. The retort will be placed near the mine so as to minimize hauling of inert rock from the mine to the retort. Before retorting, the oil shale is crushed to pieces less than 8 mm in diameter [Taciuk and Turner, 1988], and possibly less than 6 mm in practice [Schmidt, 2003].

The Alberta Taciuk Processor

The ATP retort is regarded as the most advanced above-ground retort design [Johnson, et al, 2004a]. It has low water requirements [Johnson, et al, 2004a, p. 16] and can also utilize fine shale particles, thus reducing the amount of waste shale [OSEC, 2006, p. 43]. Most or all of the retorting heat is generated through the combustion of char and produced gas, making the retorting process effectively energy self-sufficient from the point of view of the operator [Schmidt, 2003].

The ATP retort is a rotating, horizontally-oriented kiln with four main zones or chambers: pre-heat, retort, combustion, and cool-down [OSEC, 2006; Taciuk, 1981a; Taciuk et al., 1993; Taciuk and Turner, 1988]. It is classified as a hot recycled solids (HRS) retort [Burnham and McConaghy, 2006]: heat is transferred to the fresh shale from hot, already-retorted shale that is recycled into the retorting zone. The retort is operated very slightly below atmospheric pressure to prevent escape of explosive gases (-30 to -50 Pa gauge [Taciuk, 1981a]). The chambers are operated at slightly varying pressures to prevent undesired gas flow [Taciuk, 1981a, column 11]. The ATP is illustrated in Figure 3. Mass flows are labeled with lower-case letters and energy flows with upper case letters. Shale enters the retort and moves through the preheat zone (a), where it is heated to approximately 250 °C by the outgoing shale (f, Y) [Taciuk et al., 1993; OSEC, 2006]. Water contained in the shale is driven off as steam in this stage (h, Q).

The shale then moves through a seal to the retort zone (b), where it is mixed with hot, combusted shale recycled from the combustion zone (e). The combination of hot-shale recycle and conduction from the outer combustion chamber raises the temperature of the incoming shale to approximately 500 °C (W, X) [Schmidt, 2003, p. 342; Taciuk et al., 1993, column 16]. The temperature of retorting is a design characteristic, but higher temperatures result in shorter retort residence times [Hendrickson, 1975, p. 50], maximizing throughput of shale per unit of capacity built. Higher temperatures also cause somewhat higher oil and gas outputs [Hendrickson, 1975, p. 46]. There is a limit to this effect: above 600 °C there is a tendency to reduce oil yield, likely by cracking large hydrocarbons to gas [Taciuk and Turner, 1988]. Oil and non-condensable gases are removed from the retort as vapors, carrying energy with them (c, U). Non-condensable gases vary with shale

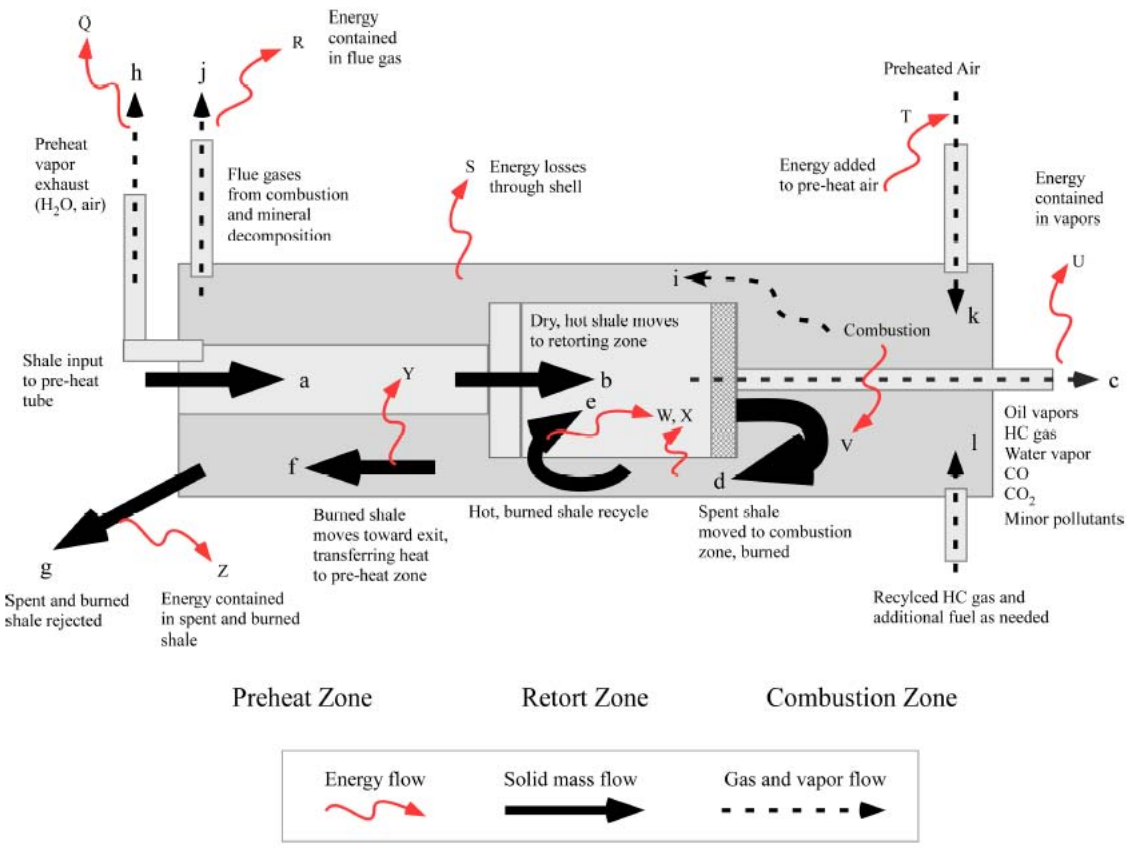

Figure 3: Schematic of mass and energy flows in the ATP retort [Taciuk, 1981, 38, Taciuk and Turner, 1988]

composition, but are approximately 35% hydrocarbons, 18% H_2, with a remainder of CO_2, CO, and H_2S [Hendrickson, 1975, p. 102]. The spent (already retorted) shale is then moved to the combustion chamber (d).

After retorting, kerogen coke or char (hydrocarbon residue deposited as nearly pure carbon) remains adhered to the spent shale. Pre-heated air and non-condensable hydrocarbon gas separated from the retort vapor output (c) are injected into the combustion chamber (k, T and l). Char and reinjected hydrocarbons are combusted at approximately 750 °C (releasing heat V) [Schmidt, 2003]. The rate of combustion is limited by air input rates [Taciuk and Turner, 1988]. The temperature of combustion is a design characteristic. Faster throughput requires higher combustion temperatures so as to more quickly transfer heat from the combusted shale to the retort zone.

The solids move back toward the inlet side of the retort, and a portion of the combusted shale is recycled into the retort (e, W). Heat is also conducted into the retort (X). The recycle rate is adjusted to maintain the correct temperature in the retorting zone [Taciuk, 1981, 1981a]. Cited recycle rates range from 60 to 80% of the shale leaving the combustion zone at any time [Taciuk, 1981, column 18].

From the combustion zone, flue gas travels (i) toward the inlet end of the retort and is removed (j, R). The shale, now spent and combusted, also moves toward the inlet end (f), transmitting heat to incoming shale in the pre-heat zone (Y). Spent shale is ejected (g) at above ambient temperature (Z). Heat loss occurs through the outer shell of the retort (S).

The ATP process is designed to provide most of the process energy from the shale char and produced hydrocarbon gas, mini-

mizing purchased energy inputs. In one case of actual operation, the vast majority (86%) of the process heat required by the retort was provided by the oil shale itself, minimizing the need for external input energy from natural gas [Schmidt, 2003].

A complication is that retorting operations can reach temperatures at which carbonate minerals within the shale decompose. The most important carbonates in Green River shale are calcite and dolomite ($CaCO_3$ and $CaMg(CO_3)_2$), which release 1 and 2 CO_2 molecules upon decomposition, respectively. These minerals, when contained in oil shale, begin decomposing at 565 °C for dolomite and between 620 °C and 675 °C for calcite ([Hendrickson, 1975], citing [Jukkola, et al., 1953]). These decomposition temperatures are significantly lower than those measured in pure mineral calcite and dolomite [Sharp, et al., 2003]. The rate of decomposition is dependent on the partial pressure of CO_2 in the air surrounding the shale particles [8]. There are a number of other minerals, mainly saline minerals (e.g. nahcolite), that decompose at retorting temperatures [Hendrickson, 1975, p. 45]. These are assumed to be present in minimal quantities in this analysis.

Post-retorting operations: disposal of spent shale, oil upgrading and refining

The spent and combusted shale is returned to a disposal location. There is some debate about swelling of oil shale after retorting (see discussion below). In the long-term, mined areas will be reclaimed.

Raw shale oil from the retort is upgraded to stabilize it and to improve its quality before it enters a refinery [OSEC, 2006, p. 100]. Sources suggest hydrotreating as the likely upgrading method [OSEC, 2006, Johnson, et al, 2004a]. The hydrotreated shale oil is sent to a refinery, likely selling at a premium to West Texas Intermediate (WTI) crude because of its high hydrogen content [Johnson, et al, 2004a, p. 32].

ATP analysis methods

Two primary cases are modeled. These represent large-scale oil shale operations, assuming large-scale mining and at least some capture and reuse of waste-heat. The high intensity case ("high case") is less optimized and uses a higher estimate for energy intensity of mining. The low-intensity case ("low case") is more optimized and has lower energy inputs to mining.

The methods and system boundaries of the ATP LCA are analogous to those used in the ICP LCA. Energy inputs and outputs are compared using same methods described above in ICP methods section, and emissions are calculated using the same methods as well. For information on detailed process-stage specific methods, see working papers mentioned above.

Results

ICP results

Total primary energy inputs and outputs per tonne of shale processed are shown in Table 1. Electricity inputs have been converted to primary energy inputs using electricity generation efficiency.

Emissions per MJ of FFD are graphed for the two primary cases in Figure 4. For

Table 1: ICP primary energy inputs and outputs per tonne of shale throughput, megajoules per tonne (MJ/tonne).

	Low case		High case	
	Inputs	Outputs	Inputs	Outputs
Preliminary operations	1		1	
Drilling	7		12	
Pumping	2		4	
Freeze wall	72		159	
Misc.	34		34	
Retorting	1168		1660	
- Oil		3377		3039
- Gas		784		480
Reclamation	39		74	
Refining	405	2971	365	2674
Total[a]	1729	3756	2309	3154

a - Total inputs are the sum of all inputs. Total output represents FFD: refined liquid product plus net gas produced.

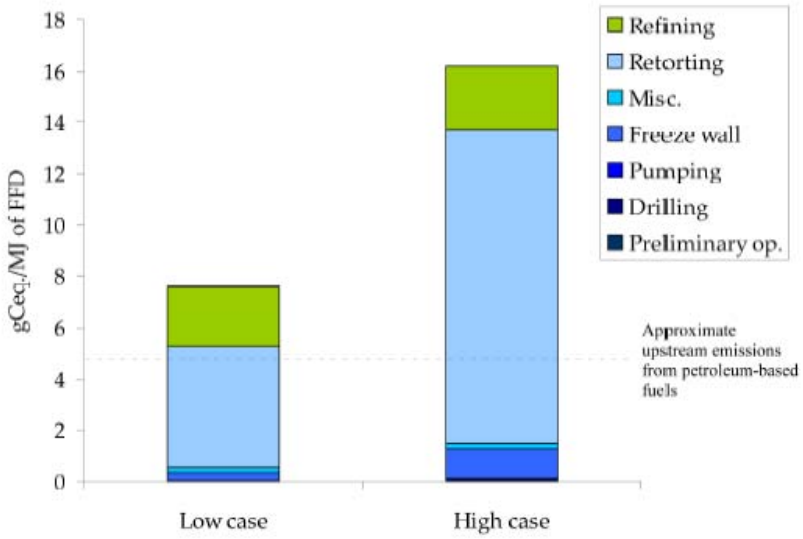

Figure 4: ICP upstream emissions from low and high primary cases, grams of carbon equivalent per megajoule of final fuel delivered (gCeq./MJ FFD).

comparison, upstream emissions from conventionally produced final fuels are roughly 5 gC_{eq}/MJ, although this can vary quite significantly depending on the final fuel produced and the production process [Brandt and Farrell, 2007; Wang, et al., 2004].

ATP results

Table 2 shows energy inputs to and outputs from each process stage per tonne of throughput in the low and high primary cases. As can be seen, energy inputs to all stages except mining, retorting, and refining are minor in comparison to energy produced.

Upstream emissions (all sources except combustion of FFD) from the primary cases are illustrated in Figure 5 in units of gC_{eq}/MJ of FFD. Note that the differences in emissions between the two primary cases are smaller than the differences in energy consumed per unit of final fuel delivered. This is because carbonate decomposition is equal in both cases, reducing the benefits of the lower energy use in the low case. Emissions from carbonate decomposition are important in both primary cases. In these cases, we calculate that 10% of calcite and 47% of dolomite are decomposed (dolomite is assumed to decompose to calcite, which then decomposes as given by calcite reaction rates [Jukkola, et al., 1953]). These decomposition figures match well with those reported for the LLNL HRS process [Burnham and McConaghy, 2006, p. 3].

5 Discussion and conclusions

The details of these two processes are uncertain in some respects, and it is unlikely that all of this uncertainty can be resolved with limited publicly available data. Despite these limitations, the energy efficiency and environmental impacts of these processes can be generally understood.

Within the calculated ranges shown above, there are reasons to expect near-term emissions from oil shale production to be closer to the high end of my reported estimates: first, the models used conservative (low) estimates of required inputs in this analysis; and second, early embodiments of new technology are rarely fully optimized. With respect to the ICP, it is possible that near-term development could be fueled with the existing grid or with incremental expansion to the existing grid and that formations may not be converted across the full depth as I assume. With respect to the ATP, it is unclear if a mature shale industry using surface mining is comparable to existing coal and tar sands

Table 2: ATP energy inputs and outputs per tonne processed (MJ/tonne throughput)

	Low case		High case		Notes
	Inputs	Outputs	Inputs	Outputs	
Preliminary operations	1.2	-	1.2	-	
Mining	202.2	-	380.8	-	
Transport	9.8	-	19.6	-	a
Crushing	11.5	-	11.5	-	b
Retort					
- Electricity	123.4	-	154.3	-	b
- Oil	-	4391.0	-	4391.0	
- Gas	213.3	100.4	250.9	62.7	
- Char	522.7	-	522.7	-	
- Waste heat	-	402.7	-	-	c
Upgrading	64.1	4089.2	87.6	4089.2	d
Refining	490.7	3598.5	490.7	3598.5	e
Total	1639	4102	1919	3661	f

a - Transport of fresh shale is 5.5 MJ/tonne in low case, transport of spent shale is about 80% of this value due to mass loss in retort.

b - MJ thermal, converted from MJ electric as described in text.

c - Input from waste heat is used in both cases to preheat combustion air, but is not counted in inputs and outputs.

d - See methods upgrading section for energy consumption and mass loss in upgrading. Inputs do not include raw shale oil energy as an input.

e - See methods for refining figures. Efficiency is 88%, inputs come from feedstock oil.

f - Total output is final fuel delivered (refined oil products, net natural gas, waste heat utilized outside of the system).

industries, especially given the significant overburden associated with some shale deposits.

Uncertainty about the ICP is larger than about the ATP [Brandt, 2007] for several reasons. First, there is more inherent flex-

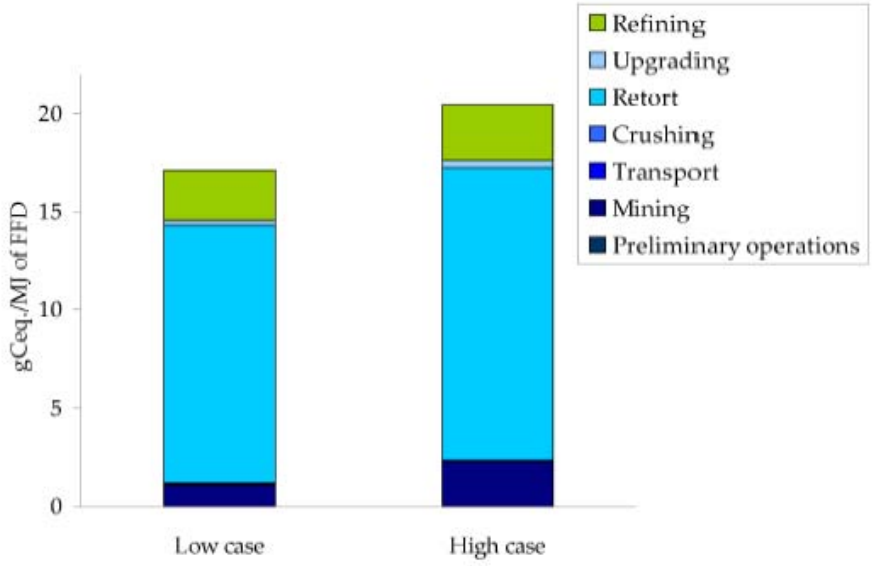

Figure 5: ATP upstream emissions from low and high primary cases, grams of carbon equivalent per MJ of final fuel delivered (gCeq./MJ FFD). Bounding cases are not presented.

ibility in the ICP than the ATP: the ATP uses a single fuel (the char from retorted shale, a high-carbon fuel), while the ICP can be used with virtually any fuel. Second, documentation of the ICP is voluminous but fragmentary, making it difficult to determine exactly how it will be implemented (at least part of this is due to experimental nature of the process). Lastly, little independent experimental work has been done at the pressures, heating rates, and other conditions proposed for the ICP.

Despite these uncertainties, results suggest that the ICP could emit fewer GHGs than above-ground mine and retort processes, such as the ATP retort [Brandt, 2007]. A broader environmental assessment is now needed, given important land use and water quality issues associated with both mining and the ICP. It is instructive to consider the implications of a very large oil shale industry. If industry were to produce, refine, and combust fuel equal to 10% of 2005 US gasoline consumption (3.3×10^8 bbl/y, or 1.8×10^{18} J [EIA, 2007]) from oil shale instead of conventional oil, full-fuel cycle emissions increase from about 45 million tonnes of carbon (MtC) for conventional oil to between 49 and 66 MtC for ICP production and between68 and 74 million tonnes of carbon for ATP production. To put these figures in perspective, emissions from all sectors in the state of Colorado equaled 24 million tonnes of carbon in 2001 [EIA, 2006]. Thus, such production could result in additional emissions commensurate with total emissions from the state of Colorado.

The wide range of potential impacts from these processes and their inherent flexibility underscores the increasing importance of deliberately and consciously choosing our path during the transition to oil substitutes. Finding an environmentally responsible path to secure domestic fuel supplies will depend not just on developing new technology to produce alternatives to oil, but also on implementing policies and programs to guide responsible deployment of that technology.

6 Acknowledgements

Alan Burnham generously provided much helpful assistance with this work. James Bartis of RAND provided feedback and assistance with calculations. Ralph Coates provided useful discussion. Richard Plevin and Alex Farrell provided helpful assistance and advice. Funding for a previous incarnation of this research was provided by the Natural Resources Defense Council.

References

Anonymous, Energy Research Stories - Alberta Innovation and Science, 2007. Available from: http://www.technology.gov.ab.ca/en/energy stories 937.cfm.

Bartis, J. T., LaTourrette, T., Dixon, L., Peterson, D. J. and Cecchine, G. Oil shale development in the United States: Prospects and policy issues. Technical report, RAND, 2005.

Berchenko, I. et al. In situ thermal processing of an oil shale formation using a pattern of heat sources. US patent number 6991032 B2, Jan 31 2006.

Berkovich, A. J., Young, B. R., Levy, J. H. and Schmidt, S. J. Thermal characterization of Australian oil shales. Journal of Thermal Analysis, 49:737–743, 1997.

U. S. Bureau of Land Management (BLM). BLM announces results of review of oil shale research nominations, January 17 2006. Available from: http://www.blm.gov/nhp/news/releases/pages/2006/pr060117 oilshale.htm%.

Brandt, A. R. Converting Green River oil shale to liquid fuels with the Alberta Taciuk Processor: energy inputs and greenhouse gas emissions, June 1 2007.

Brandt, A. R. and Farrell, A. E. Scraping the bottom of the barrel: CO_2 emission consequences of a transition to low-quality and synthetic petroleum resources. Climatic Change, Accepted for publication, March, 2007.

Burnham, A. K. Chemical kinetics and oil shale process design. Technical Report

UCRLJC- 114129, Lawrence Livermore National Laboratory, July 18-31 1993.

Burnham, A. K. Slow radio-frequency processing of large oil shale volumes to produce petroleum-like shale oil. Technical Report UCRL-ID-155045, Lawrence Livermore National Laboratory, August 20 2003.

Burnham, A. K. Personal communication with Alan Burnham regarding oil shale production, June 19 and June 28 2007.

Burnham, A. K. and McConaghy, J. R. Comparison of the acceptibility of various oil shale processes. Technical Report UCRL-CONF-226717, Lawrence Livermore National Laboratory, 2006.

Burnham, A. K. and Singleton, M. F. High-pressure pyrolysis of Green River oil shale. In Miknis, F. P. and McKay, J. F., editor, Geochemistry and chemistry of oil shales: ACS symposium series 230. American Chemical Society, Washington, D.C., 1983.

Ciambrone, D. F. Environmental life cycle analysis. Lewis Publishers, Boca Raton, Fl, 1997.

Clauser, C. and Huenges, E. Thermal conductivity of rocks and minerals. Rock physics and phase relations: a handbook of physical constants. AGU reference shelf 3., pages 105–126, 1995.

Dyni, J. R. Geology and resources of some world oil-shale deposits. Technical Report 2005-5294, US Geological Survey, US Department of the Interior, 2006.

Energy Information Administration (EIA). Emissions of greenhouse gasses in the United States 2002, Table 6-1 Carbon Coefficients. Technical report, Energy Information Administration, 2003.

EIA. State carbon dioxide emissions, 2006. Available from: http://www.eia.doe.gov/environment.html.

EIA. U.S. Product supplied for crude oil and petroleum products, Accessed May 20 2007.

U.S. Senate Energy and Natural Resources Committee (U. S. Senate). Hearing to discuss opportunities to advance technology that will facilitate environmentally friendly development of oil shale and oil sands resources, April 12th 2005.

Hendrickson, T. A. Synthetic fuels data handbook. Cameron Engineers, Inc., 1975.

Johnson, H. R., Crawford, P. M. and Bunger, J. W. Strategic significance of America's oil shale resource: Volume I - Assesment of strategic issues. Technical report, AOC Petroleum Support Services, LLC, March 2004.

Johnson, H. R., Crawford, P. M. and Bunger, J. W. Strategic significance of America's oil shale resource: Volume II - oil shale resources, technology and economics. Technical report, AOC Petroleum Support Services, LLC, March 2004. 18

Jukkola, E. E., Denilauler, A. J., Jensen, H. B., Barnet, W. I. and Murphy, W. I. R. Thermal decomposition rates of carbonates in oil shale. Industrial and Engineering Chemistry, 45(12):2711–2714, 1953. Available from: hGoto-ISIi://A1953UC53100037.

Leffler, W. L. Petroleum refining in non-technical language. PennWell Publishers, Tulsa, OK, 3rd edition, 2000.

Oil Shale Exploration Company (OSEC). Oil shale research, development, and demonstration project: White River mine, Uintah County, Utah. Technical report, Oil Sands Exploration Company and U.S. Department of the Interior, Bureau of Land Management, Vernal field office, September 18 2006.

Office of Technology Asessment (OTA). An assessment of oil shale technologies, volume 1. Congress of the United States, Office of Technology Assessment, Washington, D.C., 1980.

Sanger, F. J. and Sayles, F. H. Thermal and rheological computations for artificially frozen ground construction. Engineering geology, 13:311–377, 1979.

Schmidt, S. J. New directions for shale oil: path to a secure new oil supply well into

this century [on the example of Australia]. Oil Shale, 20(3S):333–346, 2003.

Sharp, Z. D., Papike, J. J. and Durakiewicz, T. The effect of thermal decarbonation on stable isotope compositions of carbonates. American Mineralogist, 88:87–92, 2003.

Shell. 2nd generation ICP project, oil shale research and development project plan of operation, February 15 2006. Available from: http://www.co.blm.gov/wrra/WRFO Oil shale.htm. 2006a

Shell. E-ICP test project, oil shale research and development project plan of operation, February 15 2006. Available from: http://www.co.blm.gov/wrra/WRFO Oil shale.htm. 2006b

Shell. Oil Shale Test Project, oil shale research and development project plan of operation, February 15 2006. Available from: http://www.co.blm.gov/wrra/WRFO Oil shale.htm. 2006c

Shell Frontier Oil and Gas inc. Designated mining operation reclamation permit application to Colorado Division of Reclamation and Mining Safety, Department of Natural Resources, for the Shell oil shale test project, February 9 2007.

Sundquist, E. T. and Miller, G. A. Oil shales and carbon dioxide. Science, 208(4445):740– 741, 1980.

Taciuk, W. Aparatus and process for recovery of hydrocarbon from inorganic host materials. US Patent number 4285773, August 25 1981.

Taciuk, W. Process for recovery of hydrocarbons from inorganic host materials. US patent number 4306961, December 22 1981a.

Taciuk, W. and Turner, L. R. Development status of Australian oil shale processing utilizing the Taciuk processor. Fuel, 67(10):1405–1407, 1988. Available from: http://www.sciencedirect.com/science/article/B6V3B-498MBY4-GG/2/a1d7be%184223a1bc2601c9050453ddb9.

Taciuk, W., Caple, R., Goodwin, S. and Taciuk, G. Dry thermal processor. US patent number 5217578, 1993.

Vinegar, H. Personal communication with Harold Vinegar regarding Shell ICP technology, April 6 2007.

Vinegar, H. J., Sandberg, C. L., Harris, C. K., Son, J. S., Menotti, J. L. and Carl, F. G. J. Temperature limited heaters for heating subsurface formations or wellbores. US patent application number 20040146288, July 29 2004.

Wang, M., Lee, H. and Molburg, J. Allocation of energy use in petroleum refineries to petroleum products - Implications for life-cycle energy use and emission inventory of petroleum transportation fuels. International Journal of Life Cycle Assessment, 9(1):34– 44, 2004.